Regular Article

blood

PHAGOCYTES, GRANULOCYTES, AND MYELOPOIESIS

The atypical receptor CCRL2 is required for CXCR2-dependent neutrophil recruitment and tissue damage

Annalisa Del Prete,[1,2] Laura Martínez-Muñoz,[3] Cristina Mazzon,[2] Lara Toffali,[4] Francesca Sozio,[1,2] Lorena Za,[5] Daniela Bosisio,[1] Luisa Gazzurelli,[1] Valentina Salvi,[1] Laura Tiberio,[1] Chiara Liberati,[5] Eugenio Scanziani,[6] Annunciata Vecchi,[2] Carlo Laudanna,[4] Mario Mellado,[3] Alberto Mantovani,[2,7,8] and Silvano Sozzani[1,2]

[1]Department of Molecular and Translational Medicine, University of Brescia, Brescia, Italy; [2]Humanitas Clinical and Research Center, Rozzano-Milano, Italy; [3]Department of Immunology and Oncology, Centro Nacional de Biotecnología, Madrid, Spain; [4]Department of Medicine, University of Verona, Verona, Italy; [5]Axxam Discovery Biology, Bresso, Italy; [6]Department of Veterinary Sciences and Public Health, University of Milan, Milan, Italy; [7]Laboratory of Immunology, Humanitas University, Rozzano-Milano, Italy; and [8]The William Harvey Research Institute, Queen Mary University of London, London, United Kingdom

Key Points

- CCRL2 is required for CXCR2-dependent neutrophil recruitment.
- CCRL2 forms heterodimers with CXCR2 and regulates CXCR2 signaling.

CCRL2 is a 7-transmembrane domain receptor that shares structural and functional similarities with the family of atypical chemokine receptors (ACKRs). CCRL2 is upregulated by inflammatory signals and, unlike other ACKRs, it is not a chemoattractant-scavenging receptor, does not activate β-arrestins, and is widely expressed by many leukocyte subsets. Therefore, the biological role of CCRL2 in immunity is still unclear. We report that CCRL2-deficient mice have a defect in neutrophil recruitment and are protected in 2 models of inflammatory arthritis. In vitro, CCRL2 was found to constitutively form homodimers and heterodimers with CXCR2, a main neutrophil chemotactic receptor. By heterodimerization, CCRL2 could regulate membrane expression and promote CXCR2 functions, including the activation of β2-integrins. Therefore, upregulation of CCRL2 observed under inflammatory conditions is functional to finely tune CXCR2-mediated neutrophil recruitment at sites of inflammation. (*Blood*. 2017;130(10):1223-1234)

Introduction

Leukocyte recruitment is a hallmark of inflammation and depends on the local production of chemotactic factors and on the regulation of the chemotactic receptors expressed by leukocytes.[1,2] Among chemotactic factors, chemokines represent the main family of signals able to induce leukocyte recruitment in vitro and in vivo. CXCR2 is the major chemokine receptor responsible for neutrophil recruitment. CXCR2 engagement induces the rapid $G\alpha_i$-dependent activation of phospholipase C-β, phosphatidylinositol 3-kinase γ, guanine exchange factors for Rho and ras small GTPases, talin, and kindlin-3, a signaling cascade promoting rapid β2-integrin clustering and conformational changes leading to increased affinity. This process allows the arrest and crawling of neutrophils on the surface of the endothelial cell monolayer and their extravasation.[3-5]

Atypical chemokine receptors (ACKRs) represent a small subset of proteins that express a high degree of homology with chemokine receptors. However, ACKRs lack structural determinants supporting $G\alpha_i$ signaling, making them unable to activate canonical G protein–dependent receptor signaling and cell migration.[6] At the moment, the ACKR family includes 4 proteins, namely ACKR1 (Duffy antigen receptor for chemokines), ACKR2 (D6 or CCBP2), ACKR3 (CXCR7 or RDC1), and ACKR4 (CCRL1 or CCXCKR and CCR11). In view of their ability to bind chemokines, ACKRs were shown to regulate inflammation by acting as scavenger receptors, promoting chemokine transcytosis, or regulating chemokine gradient formation.[6-9]

CCRL2 is a 7-transmembrane protein that shares some structural and functional aspects with ACKRs, such as the lack of conventional G protein–coupled receptor signaling and the inability to induce cell migration.[6,10,11] CCRL2 is expressed by barrier cells such as endothelial and epithelial cells and by a variety of leukocytes, including macrophages, dendritic cells, and neutrophils.[6,10] CCRL2 was shown to bind and present chemerin (a nonchemokine chemotactic protein) to leukocytes expressing ChemR23 (the functional chemerin receptor), a function that may be relevant for leukocyte extravasation.[12,13] CCRL2 expression is upregulated by inflammatory signals but its function remains unclear. This study investigated the role of CCRL2 in neutrophils, a leukocyte subset known to play a crucial role in the innate defense against pathogens and also involved in pathological conditions such as cancer and autoimmune disorders (eg, rheumatoid arthritis).[2,14,15] Here we report the ability of CCRL2 to regulate neutrophil migration and describe a new strategy by which atypical chemotactic receptors may control leukocyte trafficking into inflamed tissues.

Methods

Mice

CCRL2-deficient mice (knockout [KO]) (C57BL/6J)[16] did not show altered expression of other chemokine receptors and adhesion molecules (supplemental

Submitted 5 April 2017; accepted 24 July 2017. Prepublished online as *Blood* First Edition paper, 25 July 2017; DOI 10.1182/blood-2017-04-777680.

The online version of this article contains a data supplement.

The publication costs of this article were defrayed in part by page charge payment. Therefore, and solely to indicate this fact, this article is hereby marked "advertisement" in accordance with 18 USC section 1734.

Figure 1, available on the *Blood* Web site). Age- and sex-matched littermates or control C57BL/6J and DBA1 mice were purchased from Charles River Laboratory. Procedures involving animals conformed to institutional guidelines in compliance with national (D.L. N.26, 4-3-2014) and international (Directive 2010/63/EU revising Directive 86/609/EEC, September 22, 2010) law and policies.

Flow cytometry analysis

Bone marrow (BM) cells were CD16/32 (2.4G2) blocked and stained with the following monoclonal antibodies (moAbs): CD11b (M1/70), Ly6G (1A8), and F4/80 (BM8) from BD Pharmingen; anti-mouse CCRL2 (11n20) from LifeSpan BioSciences; and anti-mouse CXCR2-AlexaFluor647 (SA045E1) from Bio-Legend. Anti-ERK1/2 (T202/Y204) moAb was from BD Pharmigen. Anti-active Rac1-GTP and anti-RhoA-GTP were from NewEast Biosciences. Cells were acquired with MACSQuant (Miltenyi Biotec) or LSRFortessa flow cytometers (BD Biosciences) and were analyzed by FlowJo software.

BM neutrophil isolation

BM neutrophils were isolated by negative selection using a neutrophil isolation kit (Miltenyi Biotec). The purity of the neutrophil population was routinely more than 90% $CD11b^{+}Ly6G^{+}$ cells.

Chemotaxis

Cell migration was evaluated by using a 48-well chemotaxis chamber (Neuroprobe) and polycarbonate filters (5-μm pore size; Neuroprobe) for 50-minute incubation as described.[17] Results are expressed as number of migrated cells in an average of 5 high-power fields (100×).

Ca^{2+} mobilization

Purified neutrophils (3.75×10^6 cells per mL) were loaded with Fluo-8 No Wash dye (Catalog No. 36316, AAT Bioquest, Inc.) for 60 minutes at room temperature. Ca^{2+} mobilization in response to CXCL8 was measured by using a fluorometric-imaging plate reader ($FLIPR^{TETRA}$, Molecular Devices).

In vivo leukocyte mobilization

The recruitment of leukocytes into the peritoneal cavity after intraperitoneal administration of human CXCL8 (300 ng) or lipopolysaccharide (LPS; 15 ng)[18] at the indicated time points was analyzed in control and CCRL2-deficient mice by flow cytometry. Human CXCL8 is known to activate murine CXCR2[19] although with a lower affinity than other CXCR2 mouse ligands.[20]

Experimental arthritis

Collagen-induced arthritis (CIA) was induced in 8- to 12-week-old male CCRL2-deficient and control mice as previously described.[21] CIA was induced in DBA1 mice with 100 μg of denatured type II bovine collagen (MD Biosciences) emulsified in complete Freund's adjuvant. For the induction of serum transfer–induced arthritis (STIA), mice were intraperitoneally injected with 150 μL of serum from K/BxN transgenic mice (kindly provided by D. Mathis and C. Benoist).[22] Paws were scored for disease severity as described.[21] At the end of the experiment, the joints were removed, fixed, decalcified, and paraffin embedded. Sections (4 μm) were stained with hematoxylin and eosin and Ly6G. Antigen-induced arthritis was induced by intradermal immunization with methylated bovine serum albumin as previously described.[23] Anti-collagen antibodies in mouse sera were measured by Arthrogen-CIA enzyme-linked immunosorbent assay kit (Chondrex).[21]

BM transplantation

Control or CCRL2-deficient mice were lethally irradiated with a total dose of 9 Gy. Then, 2 hours later, mice were injected in the tail vein with 5×10^6 nucleated control or CCRL2-deficient BM cells. At 8 weeks after BM transplantation, the STIA model was performed.

Real-time polymerase chain reaction

Total RNA was extracted with RNeasy kit (Qiagen). Real-time quantitative polymerase chain reactions (PCRs) were performed on an MJ Real Time PCR system (Biorad) using an SYBR Green PCR master mix (Applied Biosystems).[16]

Underflow adhesion assay

Neutrophil behavior in underflow conditions was studied with the BioFlux 200 system (Fluxion Biosciences). First, 48-well plate microfluidics were co-coated overnight at room temperature with 2.5 μg/mL murine E-selectin and 5 μg/mL murine ICAM-1 in phosphate-buffered saline. Before use, microfluidic channels were washed with phosphate-buffered saline and then coated with 4 μM CXCL8 for 3 hours at room temperature, and the assay was performed at shear stress of 2 dyne/cm.[2,24]

Intravital microscopy

Intravital microscopy was performed in the synovial microcirculation of the mouse knee, as described.[23] Briefly, the left hind limb was placed on a stage, the patellar tendon was mobilized and partly resected, and the intraarticular knee synovial tissue was visualized. To measure the leukocyte-endothelial cell interactions, the fluorescent marker rhodamine 6G (Sigma) was intravenously injected (0.15 mg/kg) before the measurements. Images were captured with an Axiocam 503 Mono digital camera (Zeiss).

Elastase release

BM neutrophils (10^7 cells per mL) preincubated with cytochalasin B were treated with CXCL8 or CXCL1. Elastase release was determined as elastase activity measured in conditioned cell media, and fluorescence was monitored (370/460 nm, EnSightMultimode Plate Reader, PerkinElmer).

Time-lapse microscopy assay

Purified BM neutrophils were stimulated overnight with LPS, then seeded on matrigel precoated glass plates. Micropipettes (FemtotipII, Eppendorf) were loaded with 10 μL of CXCL8 (100 μg/mL) and injected at 15 hectopascals pressure. Acquisition was performed with an Axio Cam MRm monochrome digital camera (Zeiss Microscopy).

Förster resonance energy transfer experiments

For homodimer studies, HEK293 T cells were cotransfected with a constant amount of CXCR2-cyan fluorescent protein (CFP) (1.5 μg per well; 3×10^5 cells) and increasing amounts of CXCR2-yellow fluorescent protein (YFP) (0.125-4.5 μg per well)[25] or CCRL2-CFP (1 μg per well) and CCRL2-YFP (0.15-2.0 μg per well). For heterodimer determinations, CCRL2-CFP (1.5 μg per well) and CXCR2-YFP (0.25-5.5 μg per well) were used. To determine the spectral signature, cells were transiently transfected with CFP or YFP.[26] For fluorescence resonance energy transfer (FRET) determination by photobleaching, HEK293T cells were transiently cotransfected with CCRL2-CFP (0.2 μg per well; 3.5×10^4 cells)/CXCR2-YFP (0.8 μg per well). Cells (3.5×10^4 per well), cultured in coverslip chambers (Nunc) precoated with fibronectin were imaged 48 hours after complementary DNA transfection.[25] To establish the influence of CCRL2 expression on CXCR2/CXCR2 homodimers in FRET saturation curves, cells were transiently transfected with pcDNA3.1 (plasmid-coded DNA [pcDNA], empty vector) or pcDNACCRL2. At 24 hours post-transfection, these cells were cotransfected with CXCR2-CFP (1.5 μg per well; 3×10^5 cells) and CXCR2-YFP (0.125-4.5 μg per well).

Statistical analyses

Statistical analyses were performed by using Student *t* test, Mann-Whitney *U* test, and two-way analysis of variance, as appropriate. Results were analyzed by using GraphPad PRISM 5.0 software.

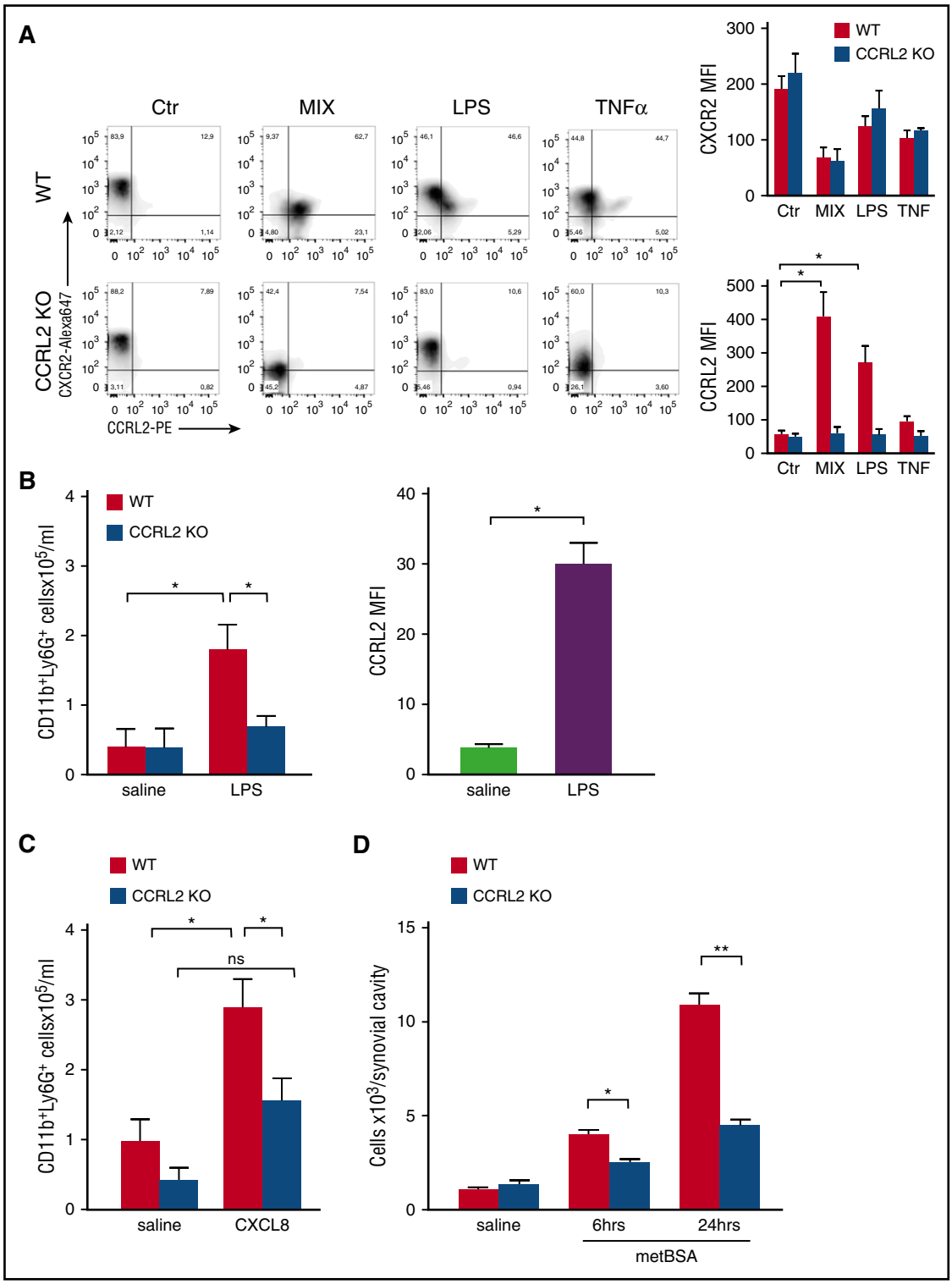

Figure 1. Defective neutrophil recruitment in CCRL2-deficient mice. (A) Cytofluorimetric profiles of CXCR2 and CCRL2 expression in purified BM neutrophils from WT and CCRL2-deficient mice (CCRL2 KO) stimulated with tumor necrosis factor α (TNF-α; 20 ng/mL), LPS (100 ng/mL), a combination of TNF-α, LPS, and 50 ng/mL interferon gamma (MIX), or medium for 18 hours. Cells were stained with a rat anti-mouse CCRL2 moAb followed by an anti-rat phycoerythrin (PE) moAb and with a rat anti-mouse CXCR2-Alexa Fluor 647 moAb. Representative plots from 3 independent experiments are shown in the left panel; right panels show summarized results of single CXCR2 and CCRL2 staining. (B-C) Peritoneal recruited cells from WT and CCRL2 KO mice injected intraperitoneally with (B) LPS (15 ng per mouse) for 2 hours or (C) CXCL8 (300 ng per mouse) for 4 hours. Control mice received sterile phosphate-buffered saline (saline). The number of $CD11b^+Ly6G^+$ neutrophils per mouse was evaluated by fluorescence-activated cell sorter analysis. The results are expressed as mean ± standard error of the mean (SEM) of 3 independent experiments for a total of 10 mice per group. (B) The rightmost graph shows mean fluorescent intensity (MFI) values of CCRL2 expression by neutrophils collected 2 hours after LPS or saline injection. (D) Cells recruited from the synovial cavity at the indicated time points after the injection of methylated bovine serum albumin (metBSA) or saline into the knee joints of metBSA-immunized mice. Results are expressed as mean ± SEM of 3 independent experiments (n = 14). $^*P < .05$; $^{**}P < .01$ by Student *t* test. ns, not significant.

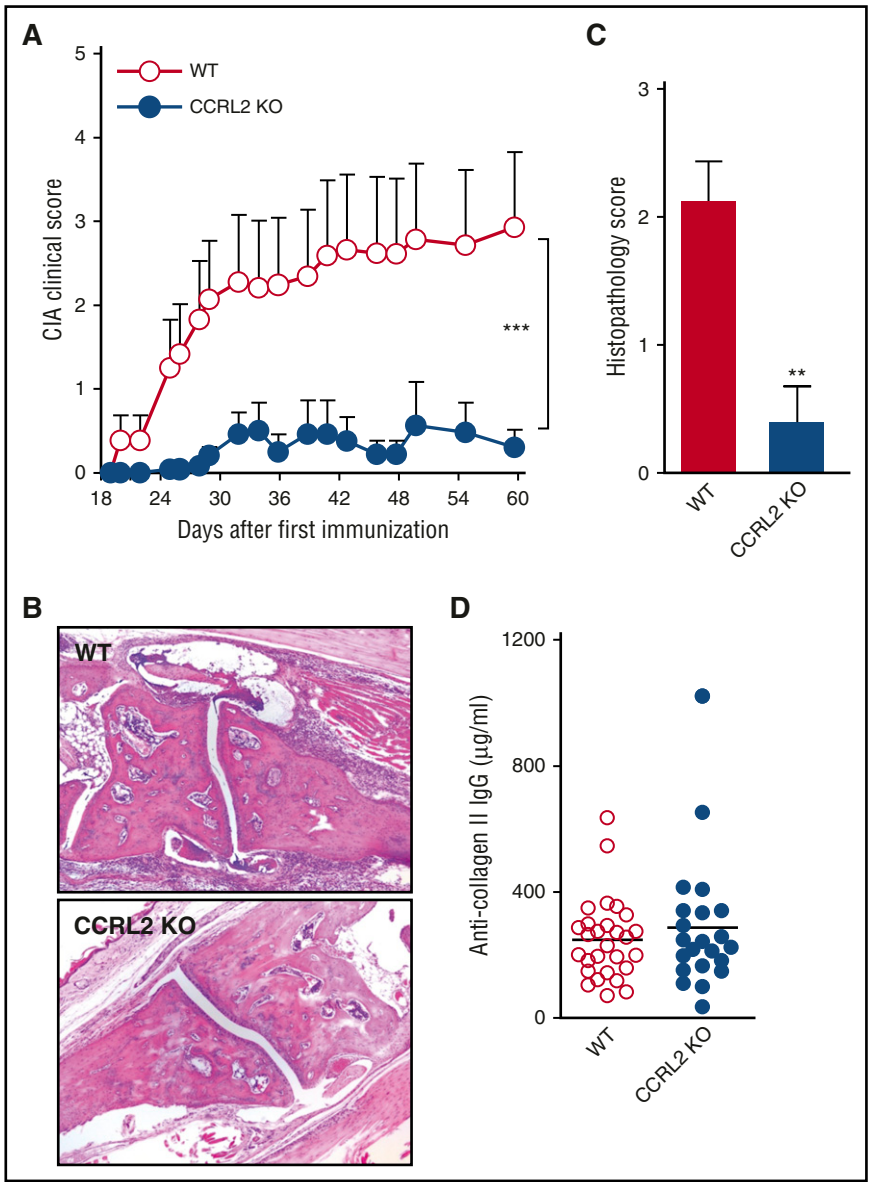

Figure 2. CCRL2-deficient mice are protected in CIA. (A) Clinical score of CIA in WT and CCRL2-deficient (KO) mice immunized with chicken type II collagen. Scores from 4 paws were combined for each mouse, and total severity score for the group was divided by the number of arthritic mice to obtain an average severity score (clinical score, 0-16 in the 4 paws). Data are shown as mean ± SEM from 1 representative experiment of 3 (WT, n = 29; CCRL2 KO, n = 24). (B) Histopathology of a representative arthritic joint from WT and CCRL2 KO mice (original magnification 4×). (C) Histopathologic score of arthritic mice as evaluated for leukocyte infiltration, erosion, pannus, necrosis/fibrosis, loss of cartilage, and bone integrity. Data are shown as mean ± SEM of arthritic scores of 1 representative experiment (WT, n = 8; CCRL2 KO, n = 10). (D) Levels of total anti-collagen II immunoglobulin G (IgG) (μg/mL) measured in mouse sera at the end of the experiment (day +60). $^{**}P < .01$ by Mann-Whitney *U* test; $^{***}P < .001$ for WT vs CCRL2 KO mice by two-way analysis of variance (ANOVA).

Results

Neutrophil recruitment is defective in CCRL2-deficient mice

Freshly isolated mouse neutrophils were found to express basal levels of membrane CCRL2. Culturing neutrophils in the absence of stimulation induced CCRL2 downregulation (105 ± 11 and 57 ± 10 representing mean fluorescent intensity ± standard error of the mean of fresh vs 18-hour-cultured neutrophils). Conversely, overnight stimulation with LPS or with the combination of proinflammatory agonists (ie, LPS, tumor necrosis factor α, and interferon gamma) caused a strong increase in CCRL2 expression with the majority of the cells co-expressing CCRL2 and CXCR2 (Figure 1A). Chemotactic agonists such as *N*-formyl-methionyl-leucyl-phenylalanine (fMLP), C5a, and CXCL8 did not regulate CCRL2 expression (data not shown). To investigate the biological role of CCRL2, neutrophil recruitment was evaluated in vivo 2 hours after the intraperitoneal injection of LPS. A marked reduction in neutrophil count was observed in CCRL2-deficient mice compared with wild-type (WT) animals (Figure 1B, left panel). Of note, at this time point, the expression of CCRL2 was already upregulated in the cells recovered from the peritoneal cavity of WT mice (Figure 1B, right panel). A marked reduction of neutrophil recruitment was also observed in response to the intraperitoneal injection of CXCL8 (Figure 1C) and after the administration of methylated bovine serum albumin into the knee joint of previously immunized CCRL2-deficient mice (Figure 1D). These results were not the result of reduced BM mobilization, because similar numbers of $CD11b^{+}/Ly6G^{+}$ cells were detected in the BM and circulation of WT and CCRL2-deficient mice after CXCL8 administration (supplemental Figure 2).

CCRL2-deficient mice are protected in experimental models of inflammatory arthritis

Different mouse models of experimental arthritis have highlighted the crucial role of neutrophils in the development of inflammatory joint diseases. Neutrophil recruitment to the inflamed joint is accomplished through the sequential activation of multiple chemokine receptors, which involves first the receptor for the lipid inflammatory mediator

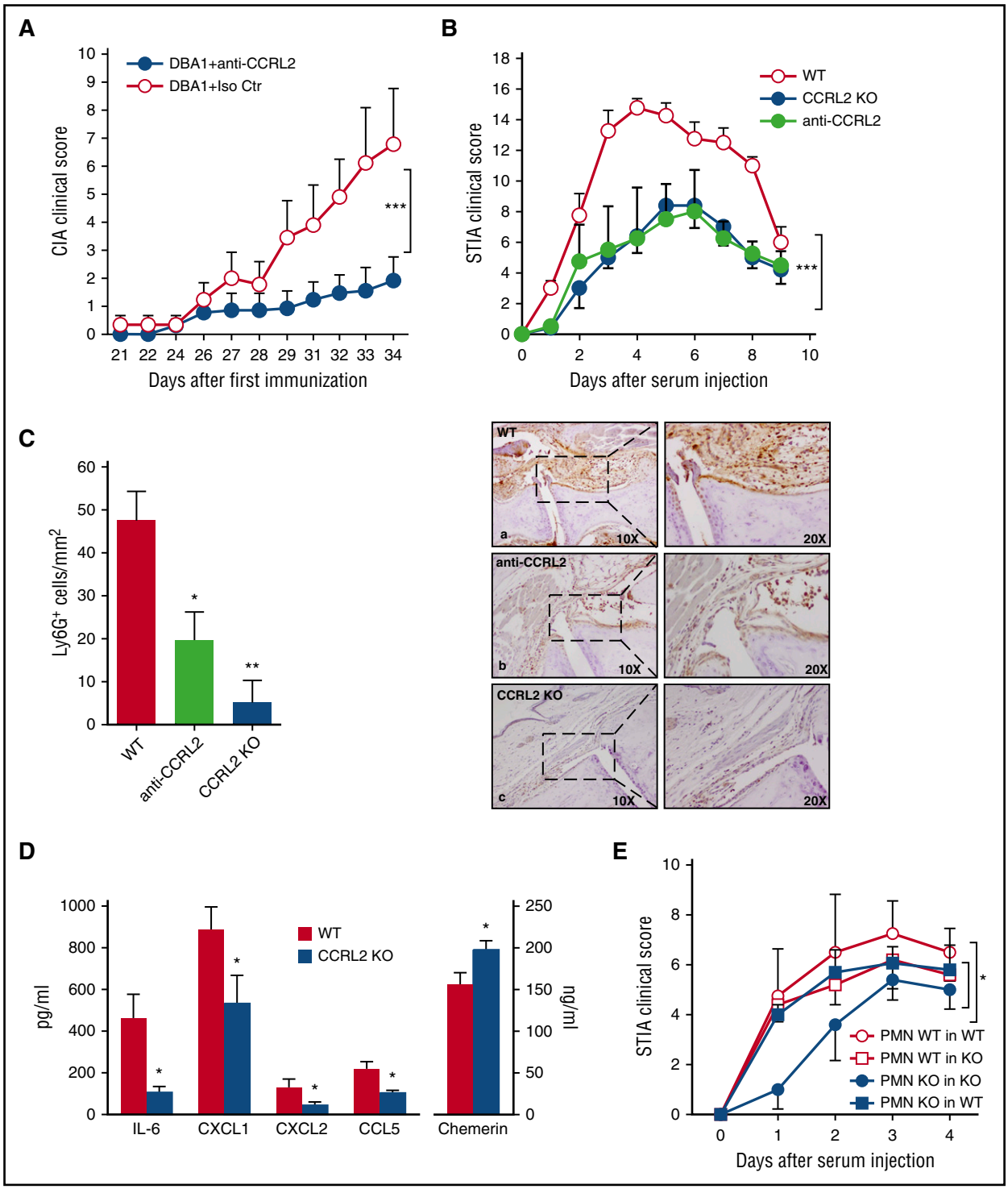

Figure 3. CCRL2-deficient mice are protected in experimental inflammatory arthritis. (A) Clinical score of CIA in DBA1 mice treated 3 times per week with anti-CCRL2 or isotype control antibody (Iso Ctr) (100 μg per mouse intraperitoneally) starting the day before the first immunization with bovine type II collagen. One representative experiment of 2 is shown. ***$P < .001$ for DBA1+anti-CCRL2 vs DBA1+Iso Ctr by two-way ANOVA (n = 10 per group). (B) Clinical score of STIA determined in CCRL2 KO, WT, and anti-CCRL2 antibody–treated WT mice (anti-CCRL2) (100 μg per mouse from day 0 to day 4). STIA was induced by injection of 150 μL of K/BxN serum at day 0 (n = 5 per group). Clinical score was assessed daily. One representative experiment of 3 is shown. ***$P < .001$ for WT vs CCRL2 KO or anti-CCRL2 group by two-way ANOVA. (C) For Ly6G staining, hyaluronidase-treated tissue sections were stained with a rat anti-mouse Ly6G antibody (BD Biosciences). Left panel: quantitative analysis of immunohistochemical staining for $Ly6G^+$ cells per mm^2 of joint sections scanned by VS120 Dot-Slide BX61 virtual slide microscope (Olympus Optical) and analyzed by using Image Pro-Premiere software (Media Cybernetics). *$P < .05$; **$P < .01$ by one-way ANOVA (n = 6 mice per group). Right panel: representative images of Ly6G staining of arthritic joints from WT, anti-CCRL2 moAb–treated WT, and CCRL2 KO mice (original magnification 10×; insets 20×). (D) Circulating levels of interleukin-6 (IL-6), CXCL1, CXCL2, CCL5, and chemerin in sera of WT and CCRL2-deficient mice at day +4 of STIA by Luminex Multiplex assay. (E) Clinical score of WT or CCRL2 KO mice receiving BM neutrophils (polymorphonuclear leukocytes [PMNs]; 5×10^6 per mouse per day) from WT and CCRL2 KO mice in STIA model. Data (n = 5 per group) from 1 representative experiment of 3 are shown. *$P < .05$ for PMN WT in WT mice or PMN WT in KO mice, or PMN KO in WT mice vs PMN KO in KO mice by two-way ANOVA.

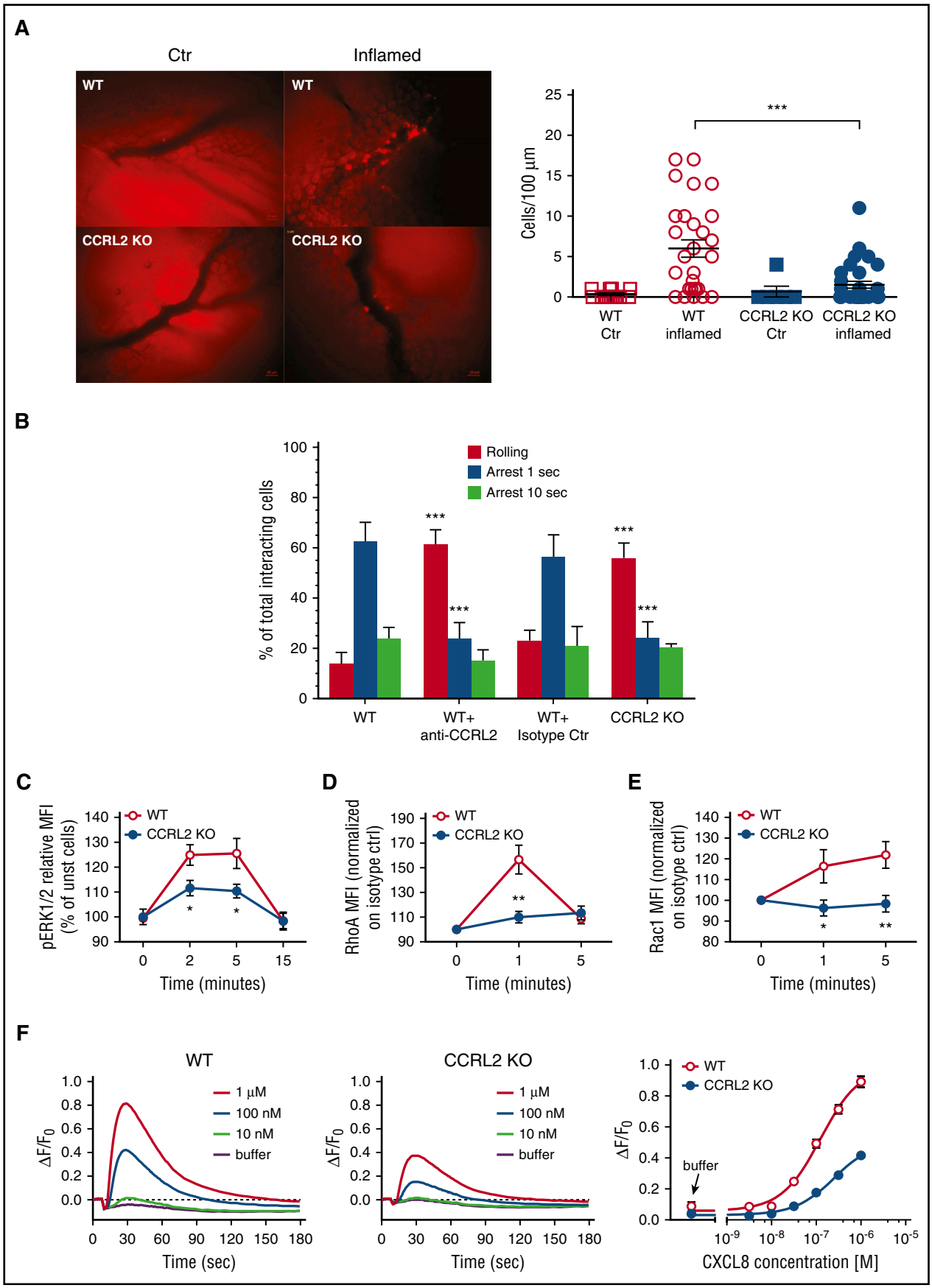

Figure 4.

leukotriene B4 (LTB4) and then the chemokine receptors CXCR1/CXCR2 and CCR1.[23,27,28]

CCRL2-deficient mice were tested first in the model of CIA to study the priming phase, which consists of the activation of the specific immune response to collagen type II and the inflammatory effector phase of the disease, which is characterized by local inflammation and cartilage and joint destruction.[29] Figure 2A shows that CCRL2-deficient mice were protected and developed arthritis with a lower incidence compared with WT controls (16.67% vs 34.48%, respectively; data not shown). CCRL2-deficient mice also showed a statistically significant delay in the onset of the disease (day +25 vs day +20 in CCRL2 KO vs WT mice, respectively) and a marked decrease in its severity. Consistent with these results, histopathologic examination highlighted a marked reduction in synovial inflammation, pannus formation, and erosion of the articular cartilage (Figure 2B-C). The reduced severity of disease observed in CCRL2-deficient mice was not associated with changes in anti-collagen type II antibody serum levels (Figure 2D), suggesting that CCRL2-associated protection is mostly confined to the inflammatory effector phase rather than the induction phase of the disease. Of interest, the repeated administration of an anti-CCRL2 moAb to DBA1 mice, a strain more susceptible to CIA (100% incidence at day 36) than C57BL/6 mice,[30] produced a degree of protection comparable to that observed in CCRL2-deficient animals (Figure 3A).

The effector phase of arthritis was further investigated by using the experimental model of the K/BxN STIA.[31] STIA is a more rapid and aggressive model than CIA; thus, it was found to be suitable for the preclinical study of new therapeutic strategies.[32] Figure 3B depicts that in this model, the appearance of the clinical symptoms was also delayed in CCRL2-deficient mice with a maximal clinical score at the peak of disease (day +4) that was only 43% of that observed in WT animals. In the STIA model, the administration of an anti-CCRL2 moAb induced a degree of protection in WT animals that was similar to that observed in CCRL2-deficient mice. Immunohistochemical analysis of $Ly6G^+$ cells revealed that neutrophil infiltration was strongly reduced in CCRL2 KO and WT mice treated with an anti-CCRL2 moAb compared with WT mice (Figure 3C). At day +4, the circulating levels of interleukin-6, a systemic marker of inflammation, were significantly reduced in CCRL2-deficient mice as were the levels of the neutrophil chemotactic cytokines CXCL1 and CXCL2 and the T-cell–attracting chemokine CCL5. As expected, on the basis of previous work,[33] in CCRL2 KO mice, serum levels of chemerin were increased by 26.7% (Figure 3D).

BM chimera obtained by WT and CCRL2-deficient BM transfer identified hematopoietic cells as the major component conferring protection in KO mice in STIA. Indeed, transplantation of CCRL2-deficient BM cells in WT mice recapitulated the protective phenotype observed in KO mice transplanted with CCRL2-deficient BM cells, whereas transplantation of WT BM cells in KO mice abolished the protective phenotype (supplemental Figure 3). Finally, adoptive transfer of WT, but not CCRL2-deficient neutrophils, abolished the protection of CCRL2-deficient mice, which identifies these cells as the main CCRL2-expressing population responsible for the protective phenotype observed in CCRL2-deficient mice (Figure 3E).

CCRL2-deficient neutrophils are defective in CXCR2-mediated signaling

To investigate the mechanisms responsible for the defective in vivo neutrophil migration, a more detailed analysis was performed by intravital microscopy using the model of methylated bovine serum albumin–induced arthritis. As shown in Figure 4A, 24 hours after the administration of the antigen into the knee of immunized WT mice, numerous cells were found to be adherent to the vessels located in the knee that received the antigen (left knee). No adherent cells were observed in the control joint (right knee) that received only saline (supplemental Movies 1 and 2). On the contrary, the inflamed joints (left knee) of CCRL2-deficient animals showed a strong reduction of endothelial cell–adherent leukocytes, with the majority of the cells undergoing the rolling process on the endothelial layer (Figure 4A; supplemental Movies 3 and 4). These results strongly suggested that CCRL2-deficient neutrophils may have a defect in integrin-mediated arrest.

To address this hypothesis, the ability of purified BM neutrophils to undergo rolling and adhesion was investigated in vitro under flow conditions. At the shear stress of 2 dyne/cm^2, which resembles the physiological shear stress normally acting in postcapillary venules, CCRL2-deficient neutrophils showed a defective ability to undergo rapid (1 second) arrest on E-selectin-, ICAM-1-, and CXCL8-coated glass capillaries. As expected, a higher number of rolling cells was counted by using CCRL2 KO neutrophils compared with WT cells (Figure 4B). This defect was best observed at the very early time points of arrest, becoming much less dramatic when the arrest parameter was set at 10 seconds, a time point more likely consistent with phenomena of postbinding stabilization and possibly outside-in signaling. Consistent with in vivo findings (Figure 3), treatment with an anti-CCRL2 moAb recapitulated the defective arrest observed with CCRL2-deficient neutrophils (Figure 4B). These findings clearly support the concurrent regulatory cooperation of CCRL2 and CXCR2 in triggering β2-integrin activation and mediated rapid arrest.

Figure 4. Defective CXCL8-dependent β2-integrin activation and signaling in CCRL2-deficient mice. (A) Intravital microscopy of the interaction between leukocytes and endothelial cells in the synovial microvasculature in WT and CCRL2-deficient (KO) mice previously immunized with metBSA. A leukocyte was considered adherent when it was stationary for at least 30 seconds, and total leukocyte adhesion was quantified as the number of adherent cells within a 100-μm length of venule in 5 minutes. Left panel: representative images captured after antigen (left) and saline (right) injection into the knees. Scale bar represents 20 μm. Right panel: quantitative analysis of cells adherent to the synovial endothelium (n = 7 mice per group). ***$P < .001$ by Student *t* test. (B) Under flow adhesion of freshly purified BM neutrophils from WT and CCRL2-deficient (KO) mice to immobilized E-selectin, ICAM-1, and CXCL8. Where indicated, WT neutrophils were pretreated with an anti-CCRL2 or isotype control moAb for 30 minutes. The behavior of interacting neutrophils was recorded on a digital drive with fast charge-coupled device video camera (25 frames per second, capable of one-half subframes per 20 millisecond recording) and analyzed subframe by subframe. Single areas of 0.2 mm^2 were recorded for at least 60 seconds. Interactions of 40 milliseconds or longer were considered significant and scored.[24] Cells that remained firmly adherent for at least 1 second were considered fully arrested. Cells arrested for at least 1 second and then detached or arrested for 10 seconds and then remained adherent were scored separately and plotted as independent groups. Data are shown as mean ± SEM of 3 experiments performed in triplicate. ***$P < .001$ WT vs CCRL2 KO or WT+anti-CCRL2 by Student *t* test. (C) ERK1/2 phosphorylation evaluated in $CD11b^+/Ly6G^+$-gated freshly isolated BM cells stimulated with 100 ng/mL CXCL8 at the indicated time points. Results are expressed as percent of increase of MFI of stimulated over unstimulated (unst) cells. Shown is the mean ± SEM for 8 mice per group in duplicates. *$P < .05$ by Student *t* test. The activation of (D) RhoA and (E) Rac1 was evaluated in $CD11b^+/Ly6G^+$-gated freshly isolated BM cells. Data are expressed as fold of increase of MFI of CXCL8 100 ng/mL stimulated over unstimulated cells (time 0) at the indicated time points. The mean ± SEM of 10 RhoA and 8 Rac1 mice per group are shown. *$P < .05$; **$P < .01$ by Student *t* test. (F) Calcium fluxes of CXCL8-stimulated WT and CCLR2-deficient neutrophils. Fluo-8 NW-loaded freshly isolated BM neutrophils were exposed to increasing concentrations of CXCL8; calcium traces are reported as $\Delta F/F_0$ above time (left 2 panels), where $\Delta F/F_0$ is the difference between the relative fluorescence units and the basal fluorescence at time 0 (F_0) normalized for F_0. Each curve represents the mean of 4 replicate wells. Right panel: concentration-response curves obtained by calculating the calcium response as $\Delta F/F_0$, where ΔF represents the difference between the maximum fluorescence signal in a selected time window (9-65 seconds) and the minimum fluorescence signal occurring at 11 seconds normalized for the basal fluorescence at F_0. Half maximal effective concentration values were 125 nM and 251 nM for WT and CCLR2-deficient neutrophils, respectively. Data are shown as mean ± SEM (n = 4). $P < .0001$ by Student *t* test.

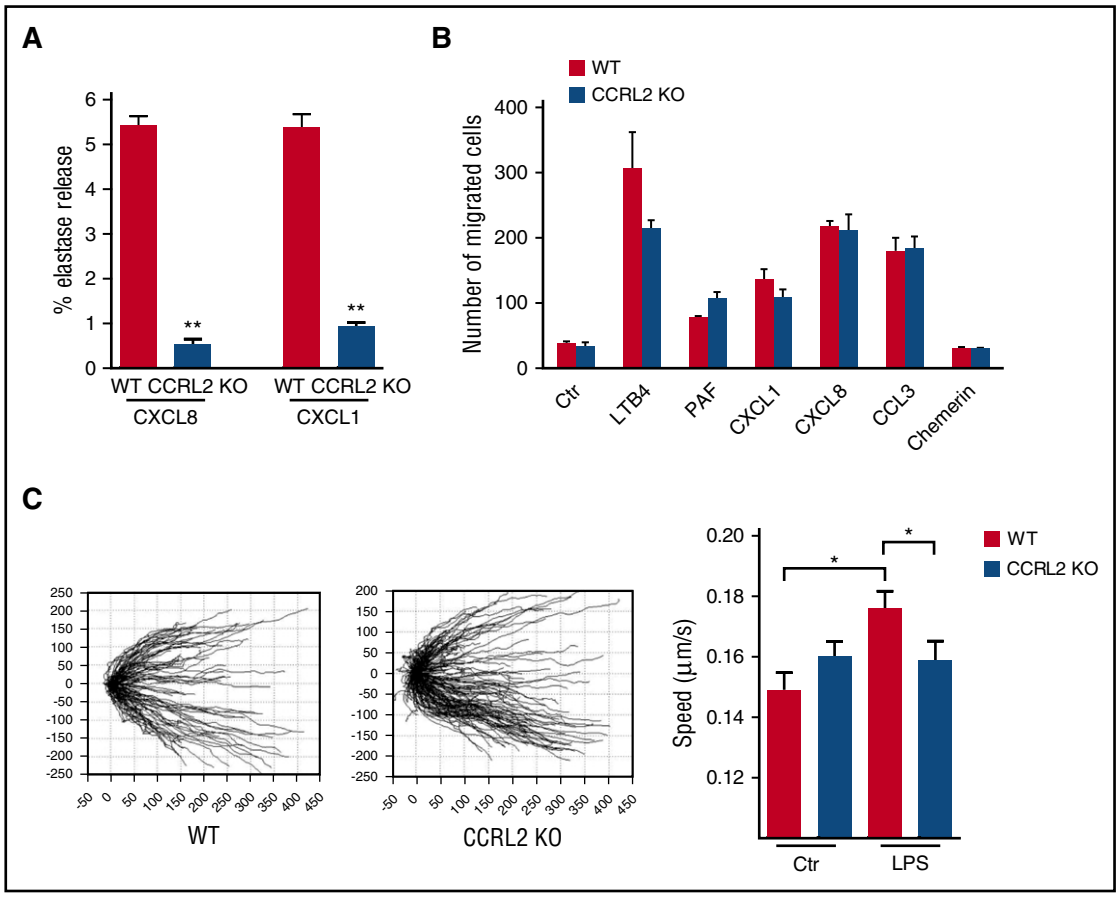

Figure 5. Role of CCRL2 in neutrophil functions. (A) Elastase release of WT and CCRL2-deficient neutrophils in response to CXCL8 and CXCL1 evaluated as elastase activity in cell supernatants. Representative results of 1 of 3 independent experiments performed in triplicate are shown as the mean ± SEM. (B) Migration of BM neutrophils in response to LTB4 (100 nM), platelet-activating factor (PAF) (100 nM), CXCL1 (100 ng/mL), CXCL8 (100 ng/mL), CCL3 (100 ng/mL), or chemerin (100 pM) evaluated in Boyden chambers as previously described.[34] Results are expressed as the mean number of migrated cells in 5 high-power fields (100×). Data are shown as the mean ± SEM of 3 independent experiments performed in triplicate. (C) Migration of BM-purified neutrophils from WT or CCRL2-deficient (KO) mice assessed by time-lapse microscopy. Representative tracking analyses of resting WT and CCRL2-deficient neutrophils in response to CXCL8 are shown in the left panel. Single-cell speed toward CXCL8 of cells stimulated with LPS (100 ng/mL) or left untreated is shown in the right panel. Single-cell directionality and speed were analyzed with ImageJ software, and data were re-elaborated by using TimeLapseAnalyser open source software (http://www.informatik.uni-ulm.de/ni/staff/HKestler/tla/). In the right panel, the mean ± SEM of the speed recorded in 3 independent experiments is shown. *$P < .05$ by one-way ANOVA; **$P < .01$ by Student t test.

To better understand the molecular basis for the defective cell adhesion, the CXCR2-mediated signaling was investigated. Stimulation of freshly isolated CCRL2-deficient neutrophils with CXCL8 produced lower levels of phospho-ERK along the entire kinetics investigated when compared with WT cells (Figure 4C). This defect was specific for CXCL8, because normal ERK1/2 phosphorylation was observed in CCRL2-deficient cells stimulated with CCL3, LTB4, or phorbol myristate acetate (supplemental Figure 4). Similarly, CXCL8-stimulated CCRL2-deficient neutrophils showed defective phosphorylation of RhoA and Rac1 small GTPases, 2 key elements in chemotactic receptor signaling (Figure 4D-E). Consistent with these results, the ability of CXCL8 to induce calcium fluxes was reduced in CCRL2-deficient neutrophils compared with WT cells starting at concentrations as low as 30 nM CXCL8 with respective 50% effective concentration values of 125.4 nM and 251.0 nM CXCL8 (Figure 4F).

CCRL2 KO neutrophils also displayed reduced release of elastase in response to CXCL8 or CXCL1, but not in response to fMLP (Figure 5A; data not shown). Conversely, neutrophil chemotaxis, investigated in vitro by using the modified Boyden chamber assay, showed a normal migration of CCRL2-deficient cells in response to a panel of chemotactic agonists, including lipids (ie, LTB4 and platelet-activating factor) and chemokines (ie, CXCL1, CXCL8, and CCL3). No migration of WT or CCRL2-deficient neutrophils was observed in response to the chemotactic protein chemerin, confirming the lack of expression of ChemR23 by both resting and activated neutrophils (Figure 5B; data not shown).[35] By using time-lapse microscopy migration assays, we showe that CCRL2-deficient neutrophils had a normal ability to orient and migrate to a CXCL8 gradient on a matrigel-coated surface (Figure 5C, left panel).[36] However, after LPS activation, which upregulates CCRL2 expression (Figure 1), CCRL2-deficient neutrophils revealed a reduced velocity in response to a CXCL8 gradient compared with WT cells. This suggests that the upregulation of CCRL2 is associated with a positive regulation of the chemotactic response to CXCL8, which is possibly related to a better interaction of WT cells with extracellular matrix components (Figure 5E, right panel).

CCRL2 and CXCR2 form both homodimers and heterodimers

Heterodimers between receptors have been proposed as a mechanism that modulates chemokine functions.[37-40] To investigate the molecular basis of CCRL2 regulation of CXCR2 signaling and function, we evaluated the possibility that these 2 receptors, when co-expressed, may form heterodimers. We generated FRET saturation

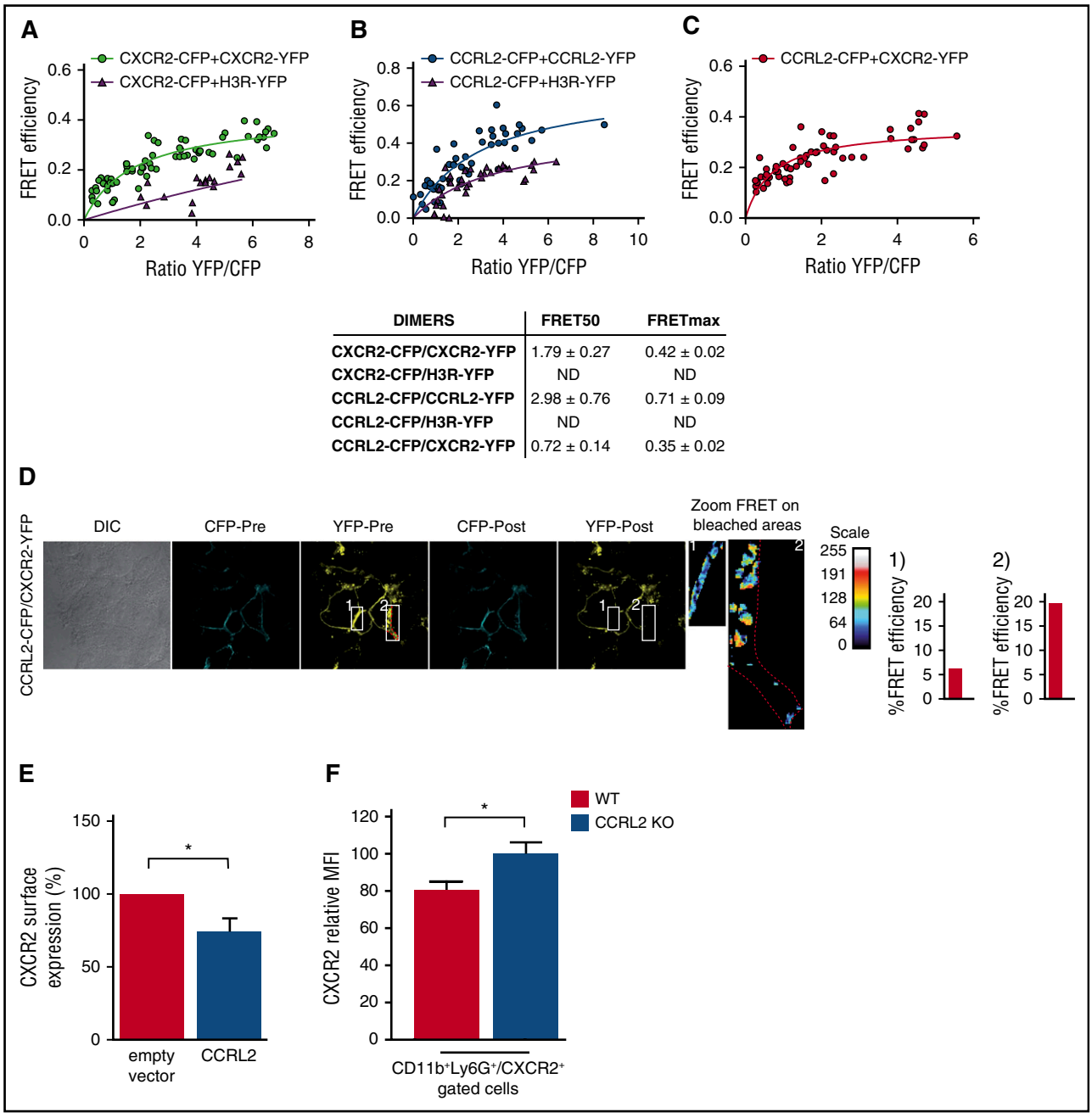

DIMERS	FRET50	FRETmax
CXCR2-CFP/CXCR2-YFP	1.79 ± 0.27	0.42 ± 0.02
CXCR2-CFP/H3R-YFP	ND	ND
CCRL2-CFP/CCRL2-YFP	2.98 ± 0.76	0.71 ± 0.09
CCRL2-CFP/H3R-YFP	ND	ND
CCRL2-CFP/CXCR2-YFP	0.72 ± 0.14	0.35 ± 0.02

Figure 6. CCRL2 and CXCR2 form homodimers and heterodimers in living cells. FRET saturation curves for (A) CXCR2/CXCR2, (B) CCRL2/CCRL2, and (C) CXCR2/CCRL2 complexes in HEK293 T cells. Curves were obtained by using cells transiently cotransfected with either the vector encoding CXCR2-CFP and increasing amounts of CXCR2-YFP plasmid or the CCRL2-CFP plasmid and increasing amounts of CCRL2-YFP plasmid. For heterodimer evaluation, we used CXCR2-CFP plasmid and increasing amounts of CCRL2-YFP plasmid. For negative controls, cells were transfected with CXCR2-CFP or CCRL2-CFP plasmid and increasing amounts of H3R-YFP plasmid. By using ImageJ 1.43u software (National Institutes of Health), FRET efficiency was determined on a pixel-by-pixel basis (E) and calculated in percent as E = [(ICFPpost – ICFPpre)/ICFPpost] × 100, where ICFPpre and ICFPpost are the background-corrected CFP fluorescence intensities before and after YFP photobleaching, respectively. FRET efficiency was calculated from ≥20 images from each of 3 independent experiments. Data are expressed as the mean ± SEM of 5 independent experiments performed in duplicate. $FRET_{50}$ and $FRET_{max}$ value were calculated by using a nonlinear regression equation for a single binding site model and are expressed as mean ± SEM (n = 5). (D) FRET analysis by acceptor photobleaching of CXCR2/CCRL2 heterodimers. Shown are representative images of CFP and YFP staining before photobleaching (CFP-Pre, YFP-Pre) and of CFP and YFP after photobleaching (CFP-Post, YFP-Post) and a zoom image of FRET at the photobleached areas (1 and 2) using a false color scale (inset). Only areas with a ~2:1 YFP:CFP ratio were selected for bleaching analysis (white outline). Areas in which the YFP:CFP ratio was unsuitable were not included in the analysis. In area 2, the red dashed line indicates the position of the cell membrane. Percentage of FRET efficiency ± SEM is shown for each photobleached area. (E) Membrane expression of CXCR2 in HEK293 T cells transfected with CXCR2 alone (empty vector) or with CCRL2 was determined by flow cytometry analysis using specific anti-CXCR2 moAb. Data are expressed as the mean ± SEM of 3 independent experiments performed in duplicate. (F) Membrane expression of CXCR2 on $CD11b^+Ly6G^+$ purified BM neutrophils from WT and CCRL2-deficient mice. Data are expressed as relative MFI (mean ± SEM of 6 mice per group). *$P < .05$ by Student t test. ND, not determined.

curves using HEK293 T cells transiently cotransfected with constant amounts of donor (CXCR2-CFP or CCRL2-CFP) and increasing amounts of acceptor (CXCR2-YFP or CCRL2-YFP). Positive FRET was observed for CXCR2 and CCRL2 homodimers (Figure 6A-B) and for CCRL2/CXCR2 heterodimers (Figure 6C). As a negative control, we used the histamine 3 receptor, which indicates the specificity of the interaction between CCRL2 and CXCR2 (Figure 6A-B).

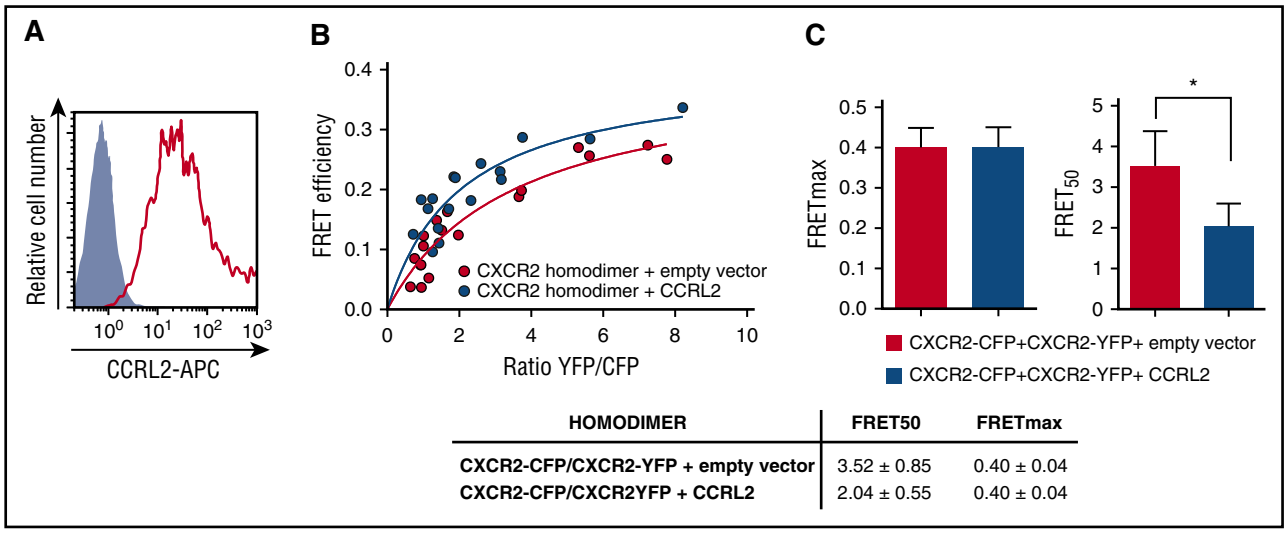

HOMODIMER	FRET50	FRETmax
CXCR2-CFP/CXCR2-YFP + empty vector	3.52 ± 0.85	0.40 ± 0.04
CXCR2-CFP/CXCR2YFP + CCRL2	2.04 ± 0.55	0.40 ± 0.04

Figure 7. CCRL2 expression modulates the CXCR2 homodimeric conformation. (A) Membrane expression of CCRL2 in HEK293 T cells transiently cotransfected with empty pcDNA3.1 (lavender) or pcDNA3.1CCRL2+CXCR2-CFP/CXCR2-YFP (red line) at a ratio of ~5 was determined by flow cytometry (stained with an anti-CCRL2 allophycocyanin [APC] conjugated Ab). CCRL2 expression is shown at a representative ratio of the curve and is maintained at all ratios tested. (B) HEK293 T cells were transiently transfected with pcDNA3.1 or pcDNA3.CCRL2. At 24 hours posttransfection, the cells were cotransfected with a constant amount of CXCR2-CFP and increasing amounts of CXCR2-YFP. A representative experiment is shown. (C) $FRET_{max}$ and $FRET_{50}$ values were deduced from data analysis by using a nonlinear regression equation applied to a single binding site model and are representative of 4 independent experiments. Data are expressed as mean ± SEM. $FRET_{50}$ values from cells co-expressing CXCR2-CFP/CXCR2-YFP + CCRL2 were significantly decreased in the 4 experiments compared with CXCR2-CFP/CXCR2-YFP+pcDNA3.1. *$P < .05$ by Student *t* test.

To corroborate these data and to determine the intracellular localization of the heterodimeric complexes, we transiently cotransfected HEK293 T cells with CCRL2-CFP (donor) and CXCR2-YFP (acceptor) at a YFP:CFP ratio at which the concentration required to achieve 50% FRET efficiency ($FRET_{50}$) signal was detected in saturation curves (Figure 6C) and determined FRET by the acceptor photobleaching method. To verify that transfection ratios corresponded to the equivalent YFP:CFP ratio determined, we measured YFP and CFP fluorescence separately in each image. CCRL2 and CXCR2 heterodimers were detected at the cell membrane and in the cytoplasm (Figure 6D), confirming heterodimerization between the 2 receptors and suggesting the existence of a pool of receptors retained intracellularly. Of note, FRET efficiency was higher for the intracellular complexes, which indicates differences in the conformation of the heterodimer depending on the cell localization evaluated. The intracellular retention of CCRL2/CXCR2 complexes was confirmed by fluorescence-activated cell sorting using an anti-CXCR2–specific moAb. The levels of CXCR2 at the cell membrane were reduced by 25.8% when HEK293 T cells were cotransfected with CCRL2 (Figure 6E). In agreement with these data, freshly isolated neutrophils obtained from CCRL2-deficient mice were characterized by a corresponding increase of membrane mean fluorescent intensity when stained with an anti-CXCR2 moAb, suggesting that KO cells express higher levels of membrane CXCR2 than WT neutrophils (Figure 6F).

CCRL2 expression modulates CXCR2 homodimeric complexes

FRET was also used to determine whether CCRL2 expression influences CXCR2 homodimer conformation. HEK293 T cells were transfected with CCRL2 or empty vector and then cotransfected with constant amounts of CXCR2-CFP (donor) and increasing amounts of CXCR2-YFP (acceptor). The CCRL2 expression was analyzed by flow cytometry at each CXCR2-YFP:CXCR2-CFP ratio (Figure 7A; data not shown). CCRL2 significantly altered FRET saturation curves for CXCR2 homodimer complexes, as indicated by the change in the $FRET_{50}$ values (3.52 ± 0.85 for CXCR2-CFP/CXCR2-YFP + pcDNA3.1 and 2.04 ± 0.56 for CXCR2-CFP/CXCR2-YFP + pcDNA3.1 CCRL2) ($P < .05$) whereas $FRET_{max}$ values were unchanged (Figure 7B-C). Energy transfer efficiency depends on the relative orientation and distance between the CXCR2-coupled fluorescent proteins; modifications in the $FRET_{50}$ values indicate changes in the apparent affinity between the 2 partners and suggest that CCRL2 co-expression alters CXCR2 homodimers.

Discussion

Inflammation is characterized by the regulated recruitment of leukocytes at the site of injury, with neutrophils usually being the first recruited cell population.[15,41] The results presented here show that the expression of CCRL2 is critical for full CXCR2 signaling and β2-integrin activation in stimulated neutrophils.

The relevance of CCRL2 upregulation under inflammatory conditions is well documented by the use of CCRL2-deficient mice in 2 models of inflammatory arthritis. These models directly rely on neutrophil recruitment.[23,27,28,42] CCRL2-deficient mice were strongly protected in terms of onset, tissue damage, and severity of the disease compared with WT animals. Of note, the administration of an anti-CCRL2 moAb to WT mice induced a degree of protection comparable to that observed in CCRL2-deficient animals. The 2 experimental models of arthritis used in this study involve the action of multiple effector cells, including macrophages and mast cells.[32] By using adoptive transfer experiments performed in the STIA model, we have excluded a role of CCRL2 expression in mast cells (data not shown), although we cannot exclude the involvement of other $CCRL2^+$ effector cells. However, because the adoptive transfer of WT neutrophils reversed the protective phenotype of CCRL2 KO mice, neutrophils are likely to be the main cell subset regulated by CCRL2 expression in STIA. CCRL2 messenger RNA was reported to be expressed by neutrophils purified from the synovial fluid of rheumatoid arthritis patients.[43] Although human neutrophils differ from their murine

counterpart in many respects, including membrane markers and cytokine production and functions,[44,45] our results show that CCRL2 is a novel potential target in rheumatoid arthritis could be exploited as a complementary therapy in low-responder patients.[46,47]

CXCR2-mediated signaling was impaired in CCRL2-deficient neutrophils, and this defect is likely to be responsible for the reduced activation of β2-integrins. In this context, it is interesting to note that β2-integrin expression on neutrophils was reported to be crucial for arthritis development in STIA.[48] In the attempt to clarify the molecular mechanisms responsible for this effect, it was observed that CCRL2 and CXCR2 form homodimers and heterodimers. CCRL2/CXCR2 heterodimerization was found to regulate CXCR2 membrane expression and signaling and to modulate the formation of CXCR2 homodimeric complexes.

GPCRs, including chemokine receptors, are known to form homodimers and heterodimers, and this process is known to regulate their functions, including intracellular trafficking and signaling pathways.[37-40,49] Two members of the ACKR family were previously reported to form both homodimers and heterodimers. ACKR1 can constitutively form heterodimers with CCR5, a receptor with which it shares the ligand CCL5.[6] The functional result of ACKR1/CCR5 heterodimerization is the inhibition of CCR5 signaling and activity.[50] Similarly, ACKR3 forms constitutive heterodimers with CXCR4, a receptor with which it shares the ligand CXCL12. The formation of ACKR3/CXCR4 heterodimers was reported to be crucial for CXCL12-induced intracellular signaling (eg, calcium flux and ERK1/2 phosphorylation).[38,39] Thus, ACKR1 and ACKR3 can form oligomers with receptors with which they share the same ligand. In this scenario, CCRL2 is apparently unique among the atypical chemotactic receptors because it forms heterodimers and regulates the function of CXCR2, the receptor for CXCL8, a chemokine that does not bind CCRL2.

Chemokines have fundamental roles in regulating immune and inflammatory responses, and during evolution, several strategies developed to control their biological activity,[6,8,51] ACKRs being 1 of those strategies. In contrast to classic chemokine receptors, ACKRs are generally expressed by non-leukocyte cell types such as barrier cells (ie, epithelial and endothelial cells) and do not activate G protein–dependent signaling.[6,8,9,52] Rather, upon binding of their ligands, ACKRs transport chemokines to intracellular degradative compartments or, in certain cell types, to the opposite side of the cell monolayer by a β-arrestin–dependent pathway.[53,54] These scavenging properties make ACKRs important molecules in the regulation of the inflammatory response.[1,9] Differing from the other ACKRs, CCRL2 is expressed by leukocytes, including macrophages, dendritic cells, mast cells, microglia, and neutrophils. In addition, CCRL2 apparently does not internalize in a constitutive manner or activate β-arrestin–dependent pathways.[10-12] Nevertheless, CCRL2 was reported to regulate the immune response in a model of immunoglobulin E–mediated cutaneous anaphylaxis and in a model of lung hypersensitivity.[12,16] In this regard, it is interesting to note that in CCRL2-deficient mice, lung dendritic cells were reported to be defective in their migration to mediastinal lymph nodes,[16] a process known to be dependent on CCR7 and CCR8.[55] Therefore, it is tempting to speculate that CCRL2 might also regulate the function of other chemokine receptors.

In conclusion, our results identify a novel pathway for regulation of neutrophil recruitment that is dependent on the expression of the atypical receptor CCRL2. We cannot formally exclude the involvement of other receptors in vivo, but our data strongly suggest that CXCR2 is a main target of CCRL2 regulation. The spectrum and structural components of CCRL2 tuning functions still remain to be fully elucidated. Nevertheless, the results obtained by using gene-modified mice and the anti-CCRL2 moAb suggest that this receptor is a potential target for inhibiting neutrophil-sustained inflammatory conditions.

Acknowledgments

The authors thank Raffaella Bonecchi for help in evaluating BM neutrophil mobilization experiments and Davide Capoferri for help with time-lapse migration experiments.

This work was supported by the European Project Innovative Medicines Initiative Joint Undertaking project BeTheCure (Contract 115142-2), Associazione Italiana Ricerca sul Cancro, Fondazione Berlucchi, Interuniversity Attraction Poles 7-40 program, and by grants from the Spanish Ministry of Economy and Competitiveness (SAF-2014-53416-R) and the RETICS Program (RD12/0009/009 RIER, RD16/0012/0006) (M.M. and L.M.-M). L.M.-M. is supported by the COMFUTURO program of the Spanish Ministry of Economy and Competitiveness General foundation. A.M. is the recipient of a European Research Council (ERC) Advanced Grant by the European Commission.

Authorship

Contribution: A.D.P., F.S., D.B., and E.S. performed and analyzed in vivo experiments; L.M.-M. and M.M. performed and analyzed FRET experiments; C.M., L.G., L. Tiberio, L. Toffali, V.S., L.Z., C. Liberati and C. Laudanna performed and analyzed in vitro experiments; A.D.P., A.V., C. Laudanna, L.M.-M., M.M., and A.M. contributed to writing and reviewing the manuscript; and S.S. planned the experiments, directed the project, and wrote the manuscript.

Conflict-of-interest disclosure: The authors declare no competing financial interests.

ORCID profiles: A.D.P., 0000-0002-3738-412X; V.S., 0000-0003-4802-1524; L. Tiberio, 0000-0003-0482-9898; E.S., 0000-0003-3996-5048; A.M., 0000-0001-5578-236X; S.S., 0000-0002-3144-8743.

Correspondence: Silvano Sozzani, Department of Molecular and Translational Medicine, University of Brescia, Viale Europa 11, 25123 Brescia, Italy; e-mail: silvano.sozzani@unibs.it.

References

1. Mantovani A, Bonecchi R, Locati M. Tuning inflammation and immunity by chemokine sequestration: decoys and more. *Nat Rev Immunol.* 2006;6(12):907-918.
2. Wright HL, Moots RJ, Edwards SW. The multifactorial role of neutrophils in rheumatoid arthritis. *Nat Rev Rheumatol.* 2014;10(10):593-601.
3. Ley K, Laudanna C, Cybulsky MI, Nourshargh S. Getting to the site of inflammation: the leukocyte adhesion cascade updated. *Nat Rev Immunol.* 2007;7(9):678-689.
4. Alon R, Ley K. Cells on the run: shear-regulated integrin activation in leukocyte rolling and arrest on endothelial cells. *Curr Opin Cell Biol.* 2008;20(5):525-532.
5. Montresor A, Toffali L, Constantin G, Laudanna C. Chemokines and the signaling modules regulating integrin affinity. *Front Immunol.* 2012;3:127.
6. Bachelerie F, Ben-Baruch A, Burkhardt AM, et al. International Union of Basic and Clinical Pharmacology. [corrected]. LXXXIX. Update on the extended family of chemokine receptors and introducing a new nomenclature for atypical

chemokine receptors. *Pharmacol Rev*. 2013; 66(1):1-79.

7. Mantovani A, Locati M, Vecchi A, Sozzani S, Allavena P. Decoy receptors: a strategy to regulate inflammatory cytokines and chemokines. *Trends Immunol*. 2001;22(6):328-336.
8. Bonecchi R, Graham GJ. Atypical chemokine receptors and their roles in the resolution of the inflammatory response. *Front Immunol*. 2016;7: 224.
9. Nibbs RJ, Graham GJ. Immune regulation by atypical chemokine receptors. *Nat Rev Immunol*. 2013;13(11):815-829.
10. Del Prete A, Bonecchi R, Vecchi A, Mantovani A, Sozzani S. CCRL2, a fringe member of the atypical chemoattractant receptor family. *Eur J Immunol*. 2013;43(6):1418-1422.
11. De Henau O, Degroot GN, Imbault V, et al. Signaling properties of chemerin receptors CMKLR1, GPR1 and CCRL2. *PLoS One*. 2016; 11(10):e0164179.
12. Zabel BA, Nakae S, Zúñiga L, et al. Mast cell-expressed orphan receptor CCRL2 binds chemerin and is required for optimal induction of IgE-mediated passive cutaneous anaphylaxis. *J Exp Med*. 2008;205(10):2207-2220.
13. Gonzalvo-Feo S, Del Prete A, Pruenster M, et al. Endothelial cell-derived chemerin promotes dendritic cell transmigration. *J Immunol*. 2014; 192(5):2366-2373.
14. Kolaczkowska E, Kubes P. Neutrophil recruitment and function in health and inflammation. *Nat Rev Immunol*. 2013;13(3):159-175.
15. Mantovani A, Cassatella MA, Costantini C, Jaillon S. Neutrophils in the activation and regulation of innate and adaptive immunity. *Nat Rev Immunol*. 2011;11(8):519-531.
16. Otero K, Vecchi A, Hirsch E, et al. Nonredundant role of CCRL2 in lung dendritic cell trafficking. *Blood*. 2010;116(16):2942-2949.
17. Del Prete A, Vermi W, Dander E, et al. Defective dendritic cell migration and activation of adaptive immunity in PI3Kgamma-deficient mice. *EMBO J*. 2004;23(17):3505-3515.
18. Hasenberg M, Köhler A, Bonifatius S, et al. Rapid immunomagnetic negative enrichment of neutrophil granulocytes from murine bone marrow for functional studies in vitro and in vivo. *PLoS One*. 2011;6(2):e17314.
19. Hirsch E, Katanaev VL, Garlanda C, et al. Central role for G protein-coupled phosphoinositide 3-kinase gamma in inflammation. *Science*. 2000; 287(5455):1049-1053.
20. Bozic CR, Gerard NP, von Uexkull-Guldenband C, et al. The murine interleukin 8 type B receptor homologue and its ligands. Expression and biological characterization. *J Biol Chem*. 1994; 269(47):29355-29358.
21. Shao WH, Del Prete A, Bock CB, Haribabu B. Targeted disruption of leukotriene B4 receptors BLT1 and BLT2: a critical role for BLT1 in collagen-induced arthritis in mice. *J Immunol*. 2006;176(10):6254-6261.
22. Kouskoff V, Korganow AS, Duchatelle V, Degott C, Benoist C, Mathis D. Organ-specific disease provoked by systemic autoimmunity. *Cell*. 1996; 87(5):811-822.
23. Coelho FM, Pinho V, Amaral FA, et al. The chemokine receptors CXCR1/CXCR2 modulate antigen-induced arthritis by regulating adhesion of neutrophils to the synovial microvasculature. *Arthritis Rheum*. 2008;58(8):2329-2337.
24. Bolomini-Vittori M, Montresor A, Giagulli C, et al. Regulation of conformer-specific activation of the integrin LFA-1 by a chemokine-triggered Rho signaling module. *Nat Immunol*. 2009;10(2): 185-194.
25. Martínez Muñoz L, Lucas P, Navarro G, et al. Dynamic regulation of CXCR1 and CXCR2 homo- and heterodimers. *J Immunol*. 2009;183(11): 7337-7346.
26. Zimmermann T, Rietdorf J, Girod A, Georget V, Pepperkok R. Spectral imaging and linear un-mixing enables improved FRET efficiency with a novel GFP2-YFP FRET pair. *FEBS Lett*. 2002; 531(2):245-249.
27. Tanaka D, Kagari T, Doi H, Shimozato T. Essential role of neutrophils in anti-type II collagen antibody and lipopolysaccharide-induced arthritis. *Immunology*. 2006;119(2):195-202.
28. Chou RC, Kim ND, Sadik CD, et al. Lipid-cytokine-chemokine cascade drives neutrophil recruitment in a murine model of inflammatory arthritis. *Immunity*. 2010;33(2):266-278.
29. Brand DD, Latham KA, Rosloniec EF. Collagen-induced arthritis. *Nat Protoc*. 2007;2(5): 1269-1275.
30. Campbell IK, Hamilton JA, Wicks IP. Collagen-induced arthritis in C57BL/6 (H-2b) mice: new insights into an important disease model of rheumatoid arthritis. *Eur J Immunol*. 2000;30(6): 1568-1575.
31. Monach PA, Mathis D, Benoist C. The K/BxN arthritis model. *Curr Protoc Immunol*. 2008; Chapter 15:Unit 15.22.
32. Christensen AD, Haase C, Cook AD, Hamilton JA. K/BxN serum-transfer arthritis as a model for human inflammatory arthritis. *Front Immunol*. 2016;7:213.
33. Monnier J, Lewén S, O'Hara E, et al. Expression, regulation, and function of atypical chemerin receptor CCRL2 on endothelial cells. *J Immunol*. 2012;189(2):956-967.
34. Bonecchi R, Facchetti F, Dusi S, et al. Induction of functional IL-8 receptors by IL-4 and IL-13 in human monocytes. *J Immunol*. 2000;164(7): 3862-3869.
35. Bondue B, Wittamer V, Parmentier M. Chemerin and its receptors in leukocyte trafficking, inflammation and metabolism. *Cytokine Growth Factor Rev*. 2011;22(5-6):331-338.
36. Jannat RA, Robbins GP, Ricart BG, Dembo M, Hammer DA. Neutrophil adhesion and chemotaxis depend on substrate mechanics. *J Phys Condens Matter*. 2010;22(19):194117.
37. Mellado M, Rodríguez-Frade JM, Vila-Coro AJ, et al. Chemokine receptor homo- or heterodimerization activates distinct signaling pathways. *EMBO J*. 2001;20(10):2497-2507.
38. Sierro F, Biben C, Martínez-Muñoz L, et al. Disrupted cardiac development but normal hematopoiesis in mice deficient in the second CXCL12/SDF-1 receptor, CXCR7. *Proc Natl Acad Sci USA*. 2007;104(37):14759-14764.
39. Levoye A, Balabanian K, Baleux F, Bachelerie F, Lagane B. CXCR7 heterodimerizes with CXCR4 and regulates CXCL12-mediated G protein signaling. *Blood*. 2009;113(24):6085-6093.
40. Barroso R, Martínez Muñoz L, Barrondo S, et al. EBI2 regulates CXCL13-mediated responses by heterodimerization with CXCR5. *FASEB J*. 2012; 26(12):4841-4854.
41. Nauseef WM, Borregaard N. Neutrophils at work. *Nat Immunol*. 2014;15(7):602-611.
42. Eyles JL, Hickey MJ, Norman MU, et al. A key role for G-CSF-induced neutrophil production and trafficking during inflammatory arthritis. *Blood*. 2008;112(13):5193-5201.
43. Galligan CL, Matsuyama W, Matsukawa A, et al. Up-regulated expression and activation of the orphan chemokine receptor, CCRL2, in rheumatoid arthritis. *Arthritis Rheum*. 2004;50(6): 1806-1814.
44. Tecchio C, Cassatella MA. Neutrophil-derived chemokines on the road to immunity. *Semin Immunol*. 2016;28(2):119-128.
45. Zschaler J, Schlorke D, Arnhold J. Differences in innate immune response between man and mouse. *Crit Rev Immunol*. 2014;34(5):433-454.
46. Udalova IA, Mantovani A, Feldmann M. Macrophage heterogeneity in the context of rheumatoid arthritis. *Nat Rev Rheumatol*. 2016; 12(8):472-485.
47. Gottenberg JE, Brocq O, Perdriger A, et al. Non-TNF-targeted biologic vs a second anti-TNF drug to treat rheumatoid arthritis in patients with insufficient response to a first anti-TNF drug: a randomized clinical trial. *JAMA*. 2016;316(11): 1172-1180.
48. Monach PA, Nigrovic PA, Chen M, et al. Neutrophils in a mouse model of autoantibody-mediated arthritis: critical producers of Fc receptor gamma, the receptor for C5a, and lymphocyte function-associated antigen 1. *Arthritis Rheum*. 2010;62(3):753-764.
49. Thelen M, Muñoz LM, Rodríguez-Frade JM, Mellado M. Chemokine receptor oligomerization: functional considerations. *Curr Opin Pharmacol*. 2010;10(1):38-43.
50. Chakera A, Seeber RM, John AE, Eidne KA, Greaves DR. The duffy antigen/receptor for chemokines exists in an oligomeric form in living cells and functionally antagonizes CCR5 signaling through hetero-oligomerization. *Mol Pharmacol*. 2008;73(5):1362-1370.
51. Rot A, von Andrian UH. Chemokines in innate and adaptive host defense: basic chemokinese grammar for immune cells. *Annu Rev Immunol*. 2004;22:891-928.
52. Bonecchi R, Savino B, Borroni EM, Mantovani A, Locati M. Chemokine decoy receptors: structure-function and biological properties. *Curr Top Microbiol Immunol*. 2010;341:15-36.
53. Colditz IG, Schneider MA, Pruenster M, Rot A. Chemokines at large: in-vivo mechanisms of their transport, presentation and clearance. *Thromb Haemost*. 2007;97(5):688-693.
54. Borroni EM, Cancellieri C, Vacchini A, et al. β-arrestin-dependent activation of the cofilin pathway is required for the scavenging activity of the atypical chemokine receptor D6. *Sci Signal*. 2013;6(273):ra30.1-11, S1-3. doi: 10.1126/scisignal.2003627
55. Jakubzick C, Tacke F, Llodra J, van Rooijen N, Randolph GJ. Modulation of dendritic cell trafficking to and from the airways. *J Immunol*. 2006;176(6):3578-3584.